Archival Report

Biological Psychiatry: CNNI

Alterations of Functional Connectivity Dynamics in Affective and Psychotic Disorders

Linnea Hoheisel, Lana Kambeitz-Ilankovic, Julian Wenzel, Shalaila S. Haas, Linda A. Antonucci, Anne Ruef, Nora Penzel, Frauke Schultze-Lutter, Theresa Lichtenstein, Marlene Rosen, Dominic B. Dwyer, Raimo K.R. Salokangas, Rebekka Lencer, Paolo Brambilla, Stephan Borgwardt, Stephen J. Wood, Rachel Upthegrove, Alessandro Bertolino, Stephan Ruhrmann, Eva Meisenzahl, Nikolaos Koutsouleris, Gereon R. Fink, Silvia Daun, and Joseph Kambeitz, for the PRONIA Consortium

ABSTRACT

BACKGROUND: Patients with psychosis and patients with depression exhibit widespread neurobiological abnormalities. The analysis of dynamic functional connectivity (dFC) allows for the detection of changes in complex brain activity patterns, providing insights into common and unique processes underlying these disorders.

METHODS: We report the analysis of dFC in a large sample including 127 patients at clinical high risk for psychosis, 142 patients with recent-onset psychosis, 134 patients with recent-onset depression, and 256 healthy control participants. A sliding window–based technique was used to calculate the time-dependent FC in resting-state magnetic resonance imaging data, followed by clustering to reveal recurrent FC states in each diagnostic group.

RESULTS: We identified 5 unique FC states, which could be identified in all groups with high consistency (mean r = 0.889 [SD = 0.116]). Analysis of dynamic parameters of these states showed a characteristic increase in the lifetime and frequency of a weakly connected FC state in patients with recent-onset depression ($p < .0005$) compared with the other groups and a common increase in the lifetime of an FC state characterized by high sensorimotor and cingulo-opercular connectivities in all patient groups compared with the healthy control group ($p < .0002$). Canonical correlation analysis revealed a mode that exhibited significant correlations between dFC parameters and clinical variables (r = 0.617, $p < .0029$), which was associated with positive psychosis symptom severity and several dFC parameters.

CONCLUSIONS: Our findings indicate diagnosis-specific alterations of dFC and underline the potential of dynamic analysis to characterize disorders such as depression and psychosis and clinical risk states.

https://doi.org/10.1016/j.bpsc.2024.02.013

Psychotic and affective disorders are both prevalent and highly disruptive to patients' quality of life, making these disorders some of the most important contributors to global disease burden (1). Understanding the pathophysiology underlying these disorders through neuroimaging might facilitate the development of tools for early diagnosis or the identification of novel interventions (2,3). The analysis of connectivity between brain regions, particularly dynamic functional connectivity (dFC), has proven to be an effective method of characterizing brain alterations in health and disease (4,5). Studying dFC abnormalities in patients with psychiatric disorders could reveal important information on brain changes associated with psychiatric symptoms and provide indications of their mechanisms.

The discovery of the behaviorally meaningful network structure of brain FC at rest (6,7) spurred numerous investigations of FC in patients with a range of brain disorders, including psychosis and depression (8,9). Several more recent studies have also examined changes in FC in patients at clinical high risk (CHR) for psychosis (10–12), a prodromal stage that often precedes a full psychotic disorder. This population is particularly interesting because pathophysiological processes can be investigated before potential effects of treatment, hospitalization, and disability are consolidated (13). Since there is significant clinical overlap between patients with depression, patients with psychosis, and patients at CHR for psychosis (2,14), comparing brain changes between these groups might provide insights into diagnosis-specific disease processes.

Studies of static, or time-averaged, functional brain connectivity indicate robust alterations in patients with depression (15,16) and patients with psychosis (17,18). Aberrant connectivity patterns particularly in the default mode network (DMN), central executive network, and salience network have been identified in both affective and psychotic disorders, but the specific patterns of abnormalities differ between diagnoses

© 2024 Society of Biological Psychiatry. Published by Elsevier Inc. This is an open access article under the CC BY license (http://creativecommons.org/licenses/by/4.0/).

ISSN: 2451-9022 Biological Psychiatry: Cognitive Neuroscience and Neuroimaging August 2024; 9:765–776 www.sobp.org/BPCNNI

(19,20). While patients with psychosis exhibit reduced FC both within the DMN and between the DMN and salience network (21), studies show an increase in FC in these networks and a decrease in connectivity between the DMN and central executive network in patients with depression (16). Communication between cortical and subcortical areas is also disturbed in both disorders, with alterations in FC commonly found between subcortical structures such as the striatum and areas in the prefrontal cortex (22,23). The same brain networks are likewise affected in patients at CHR for psychosis (24), although a differentiation between psychotic, affective, and CHR-specific changes is lacking.

However, analyses of static FC are limited as they neglect the time-dependent variability of brain network connectivity. These techniques cannot uncover alterations in FC in patients with psychiatric disorders that occur only in the temporal domain. Since research suggests that dynamic properties of FC change in depressive and psychotic disorders (4,25–27), examination of these properties might reveal symptom-related and transdiagnostic brain abnormalities. One powerful approach to detecting temporal alterations of brain connectivity is based on computing FC within sliding windows. This allows for the identification of recurrent FC states, which are characterized by specific patterns of correlated activity between brain regions or brain networks (28,29). The characteristics of such FC states are promising potential biomarkers of psychotic and affective disorders and reveal information about changes in transient brain activity and mechanisms that cannot be gained from static FC alone (5,30).

The analysis of dynamic connectivity has so far been limited to studies with small sample size and provided heterogeneous findings (4,5,31,32). Some initial findings suggest an overall decrease in temporal variability in depression (33), with patients spending a longer time in a weakly connected state (4). In contrast, patients with psychosis spend less time in states characterized by high connectivity within and between sensory areas and more time in states with high connectivity within the DMN (25). Moreover, other studies indicate that psychosis is associated with temporal disconnectivity (30,34). The limited data available on dFC changes in patients at CHR for psychosis indicate not only some overlap of abnormalities with patients with psychosis in the connectivity pattern of a dominant FC state, but also variations specific to the prodromal state (27). It is still unclear, however, to what extent those findings are related to psychotic symptoms, rather than to a general burden of disease or affective symptoms that both patients at CHR and patients with psychosis commonly experience. Due to the wide variety of methodologies employed in dFC analyses (28), comparing results across studies remains challenging, which makes it particularly important to contrast patients at CHR, patients with psychosis, and patients with depression with each other as well as with healthy control (HC) individuals.

In the present work, we provide first results from a large-scale neuroimaging study of patients at CHR of psychosis, patients with recent-onset psychosis (ROP), patients with recent-onset depression (ROD), and HC participants. We investigated dFC changes by combining the sliding window method with a consensus clustering approach to identify a set of FC states. We then compared the dFC features of these states, specifically lifetimes, frequencies, and transition frequencies, across diagnostic groups. We investigated their relationship with clinical variables such as symptom severity, level of functioning, and cognitive scores with the aim of identifying specific and transdiagnostic alterations in dFC.

METHODS AND MATERIALS

Participants

The PRONIA (Personalised Prognostic Tools for Early Psychosis Management; www.pronia.eu) study is a multicenter, naturalistic longitudinal study including patients with ROP, patients with ROD, patients at CHR for psychosis, and HC participants. A comprehensive baseline assessment including a detailed clinical characterization, neurocognitive testing, blood sampling, and a multimodal neuroimaging protocol (structural magnetic resonance imaging [MRI], resting-state functional MRI [fMRI], diffusion tensor imaging) was conducted in all study participants. All participants were invited for follow-up examinations over a period of 36 months. Further details regarding the study design are provided in previous publications (35,36). All adult study participants provided written informed consent before inclusion in the study. Minor participants (younger than 18 years of age) provided assent, and written informed consent was obtained from their guardians. The study was registered at the German Clinical Trials Register (DRKS00005042) and approved by the local research ethics committees in each study center. Patients with ROD and ROP were included in the study if they met criteria for the respective diagnosis within the past 3 months according to the Structured Clinical Interview for DSM-IV-TR (37) and the current episode did not last longer than 24 months. Patients at CHR for psychosis were included in the study if they fulfilled cognitive disturbances criteria as assessed by the Schizophrenia Proneness Instrument, Adult Version (38) or ultra-high-risk criteria for psychosis as assessed by the Structured Interview for Psychosis-Risk Syndromes (39). Further details on inclusion and exclusion criteria are available in the Supplement.

Clinical Assessment

The clinical assessment of study participants included the Beck Depression Inventory–II (40), the Positive and Negative Syndrome Scale (PANSS) (41), the Global Functioning: Role Scale (42) and Global Functioning: Social Scale (43) for global role and social functioning, and the Global Assessment of Functioning (44). In addition, types and dosages of psychiatric medications were recorded.

MRI Acquisition and Preprocessing

All participants underwent multimodal neuroimaging including acquisition of structural and resting-state fMRI. T1 reference images were acquired using a multiecho magnetization-prepared rapid acquisition gradient-echo sequence with the following parameters: repetition time = 9.5 ms, echo time = 5.5 ms, 8° flip angle, 250 × 250 mm^2 field of view, 256 × 256 matrix size, 190 contiguous sagittal slices of 1.0-mm thickness and 1.0-mm gap, 0.97 mm × 0.97 mm × 1 mm voxel size, and pixel band width = 650 Hz. Blood oxygenation level–

dependent images of the whole brain were acquired using an echo-planar imaging sequence with 53 ascending slices (repetition time = 3000 ms, echo time = 30 ms, 90° flip angle, 230 × 230 mm^2 field of view, 3.0-mm thickness and 3.0-mm gap, 80 × 80 matrix size, 2.875 mm × 2.875 mm × 3 mm voxel size) using the intercommissural line (anterior commissure-posterior commissure) as a reference. Resting-state fMRI scans resulted in 200 volumes (603-second duration), and participants were instructed to keep their eyes open during the scan.

T1 structural MRI images were preprocessed using CAT12 (https://www.neuro.uni-jena.de/cat12) (45). Resting-state fMRI preprocessing steps comprised realignment, coregistration, warping to Montreal Neurological Institute space and smoothing, motion correction by time series despiking with the Brain Wavelet Toolbox (46), background filtering, temporal bandpass filtering (0.01–0.08 Hz), signal extraction from white matter and cerebrospinal fluid, and calculation of framewise displacement for each participant to determine inclusion (47). The preprocessed volumes were parcellated using the 160-region Dosenbach atlas (48). Details of the preprocessing procedure are available in the Supplement.

dFC Analysis

We obtained time-resolved FC for each participant using the sliding window method (49) (Figure 1). For a given time window, we calculated the Pearson correlation coefficient of brain activity between each pair of brain areas, yielding a 160 × 160 FC matrix. We selected a window length of 30 repetition times, or 90 seconds, which has been recommended for dynamic connectivity analysis (50,51). Since conventional sliding window analysis considers data points only within the window, peaks in brain activity can lead to large changes in FC between subsequent windows as they enter or exit the range of data points under consideration. To reduce this effect, we calculated a weighted correlation using a Gaussian kernel (σ = 3), allowing data points to move into and out of the window gradually (52). Subsequently, the window was shifted by an offset of 1 frame, and new correlation coefficients were determined. This process was repeated until the last frame was reached, resulting in 162 FC matrices. We applied the Fisher z transformation to the correlation coefficients, yielding an approximately normally distributed feature. Since FC matrices are symmetrical and the correlation of the activity in each area with itself is always perfect, we conducted further analyses on the 12,720 elements of their upper triangulars excluding the diagonal. Thus, for each participant, we obtained a matrix of size 162 × 12,720 representing the 12,720 pairwise FCs between brain regions for a total of 162 time points.

In accordance with previous studies (29), we identified a set of recurrent brain states for each diagnostic group and the HC group individually using k-means clustering and a consensus clustering approach. Here, k-means clustering was conducted 10 times, and results were aggregated to improve the reliability of the clustering solution. We calculated the rate at which 2 FC vectors were assigned to different clusters for each pair of matrices in our data. The resulting matrix served as a distance estimation for an agglomerative hierarchical clustering algorithm, which produced the final consensus clustering assignment. Since there is no consensus on the optimal number of FC states, with different studies identifying between 2 (4) and 5 (53) states, we explored a range of partition models comprising between 2 and 10 states and computed a set of clustering quality metrics. First, we performed a split-half analysis, clustering the first and second halves of HC scans separately. We then determined the correlation between the means of first-half and matching second-half states, identifying values for k that yielded states with high consistency between the samples. In addition, we determined the Davies-Bouldin (54) and the Calinski-Harabasz (55) scores.

Differences in dFC in CHR, ROD, and ROP Groups

As brain states were identified separately for HC, ROD, ROP, and CHR groups, we performed a matching procedure to establish correspondence between brain states across diagnostic groups. Here, similarity between 2 brain states was quantified by the correlation between the state means. The pairwise similarity for each brain state was computed for each patient group (CHR, ROD, and ROP) relative to the HC group, which resulted in 3 similarity matrices (CHR vs. HC, ROD vs.

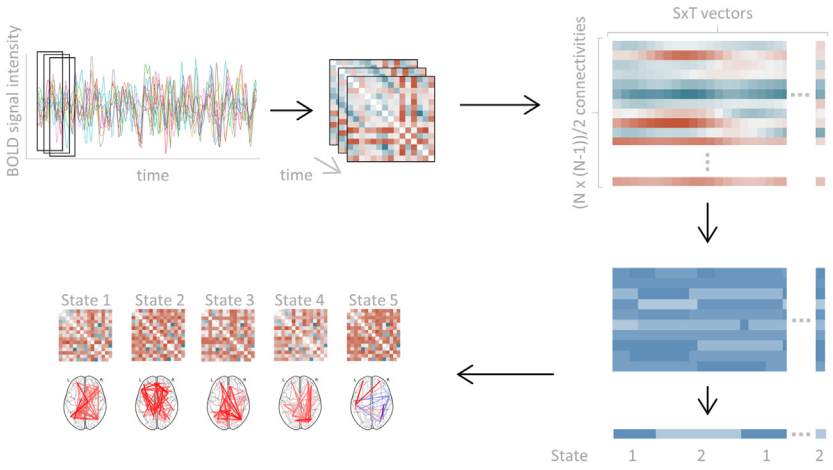

Figure 1. Generation of time-resolved functional connectivity (FC). Using a sliding window technique, FC matrices representing pairwise correlations between brain regions were computed for each time window. The upper triangulars of the FC matrices for each time window for each subject were combined into 1 matrix. K-means clustering was performed repeatedly, and a clustering consensus was derived. Based on the clustering solution, unique FC states were identified and characterized. BOLD, blood oxygenation level–dependent; S×T, subjects × time points.

HC, ROP vs. HC). In each matrix, we selected the pair of states with the highest correlation and assigned the state identified in the patient group to the corresponding HC state. The correlation values of both states to all other states, i.e., the row and column in the similarity matrix that contained the highest value in their intersection, were then set to 0. The process was repeated until all states identified in the patient group were assigned a corresponding HC state. In addition, we calculated the average connectivities within and between the resting-state networks identified by Dosenbach *et al.* (48), as well as the average connectivities within cortical, subcortical, and cortico-subcortical links, of each HC state mean to better characterize the FC states we identified.

For each participant group and each brain state, we computed 1) state lifetimes (the average amount of time spent in the state until transition to the next state), 2) state probabilities (the percentage of time participants spent in the state), and 3) transition frequencies (the number of times each state switches into another state) (28). We transformed the parameters to a normal distribution using the Yeo-Johnson transformation and removed gender, age, and site effects, as well as motion effects related to mean framewise displacement, via confound regression. Then, we compared the 4 participant groups with respect to these metrics employing Mann-Whitney *U* tests. We further analyzed the network described by the transition frequencies and compared the in-degree, i.e., the total number of transitions into each state, between groups.

Association With Clinical Variables

Subsequently, we employed canonical correlation analysis (CCA) (56,57) to relate patterns of dFC features represented by the brain states to clinical variables and to identify transdiagnostic brain-behavior relationships in the patient groups. We considered lifetimes, frequencies, and transition frequencies for each state or pair of states as dFC features and symptom severity, demographic variables, and cognitive domain scores as clinical features. Missing values in one of the clinical variables were replaced with a groupwise median. Participants with more than one missing value were excluded from the analysis. To determine the statistical significance of the correlation between the 2 variates, as well as between each variate and the associated features, we performed permutation-based hypothesis testing. We generated 1000 versions of the original dataset but randomized the order of the dFC features and clinical features. Then, CCA was applied to identify modes that highly correlate between each randomized dataset and the original data, producing distributions of correlation values for each component against which the original correlations were tested.

RESULTS

Sample Description

Of the 688 participants in the dataset, 4 were excluded due to missing data, and another 14 were excluded due to excessive motion during the fMRI scan. Therefore, 261 HC participants, 130 patients at CHR for psychosis, 143 patients with ROP, and 136 patients with ROD were included in the present analysis (Table 1). There were significant differences in the age and

Table 1. Sample Demographics

	HC Group, *n* = 261	CHR Group, *n* = 130	ROP Group, *n* = 143	ROD Group, *n* = 136	χ^2/t Value	*p* Value	HC vs. CHR		HC vs. ROP		HC vs. ROD		CHR vs. ROP		CHR vs. ROD		ROP vs. ROD	
							χ^2 Value	*p* Value	χ^2 Value	*p* Value	χ^2 Value	*p* Value	χ^2 Value	*p* Value	χ^2 Value	*p* Value	χ^2 Value	*p* Value
Gender, Male/Female, *n*	105/156	67/63	87/56	59/77	17.511[a]	.001	4.057	.044	14.919	<.001	0.248	.618	2.032	.154	1.461	.227	7.830	.005
Age, Years, Mean (SD)	28.9 (6.4)	27.1 (5.0)	28.6 (5.4)	29.1 (6.4)	9.055	.029	19673.5	.010	18746.5	.940	17357.5	.719	7688.0	.013	7251.0	.011	9481.5	.719
Medication, Daily Dose in CPZE, Mean (SD)	–	20.2 (56.1)	374.4 (932.7)	23.1 (108.8)	285.336	<.001	13702.5	<.001	5742.0	<.001	14877.0	<.001	3883.0	<.001	9125.0	.495	15550.0	<.001
PANSS Positive Scale, Mean (SD)	–	11.4 (3.4)	19.0 (5.9)	8.3 (1.7)	231.306	<.001	–	–	–	–	–	–	2344.0	<.001	13528.0	<.001	17350.5	<.001
PANSS Negative Scale, Mean (SD)	–	12.4 (6.9)	16.2 (10.7)	12.4 (6.7)	24.166	<.001	–	–	–	–	–	–	6107.5	<.001	8011.5	.468	11530.0	<.001
PANSS General Scale, Mean (SD)	–	27.8 (5.8)	35.5 (7.8)	27.3 (4.8)	58.662	<.001	–	–	–	–	–	–	4848.5	<.001	8597.0	.724	13332.5	<.001
BDI-II, Mean (SD)	3.5 (5.0)	25.9 (12.5)	21.2 (12.4)	26.2 (13.9)	351.716	<.001	1445.5	<.001	2579.5	<.001	1379.0	<.001	9064.5	.002	7369.0	.753	6087.5	.011
GAF Disability/Impairment, Mean (SD)	85.2 (6.4)	56.2 (13.7)	45.2 (12.1)	56.4 (14.7)	462.127	<.001	32740.5	<.001	36500.0	<.001	34112.0	<.001	13520.0	<.001	8673.5	.871	5227.5	<.001
GAF Symptoms, Mean (SD)	86.7 (6.4)	55.0 (11.0)	40.9 (13.1)	55.6 (11.9)	499.402	<.001	33528.0	<.001	36630.0	<.001	34548.0	<.001	14641.0	<.001	8505.0	.665	3780.5	<.001
EHI, Mean (SD)	75.8 (45.6)	66.7 (57.6)	70.4 (53.8)	75.6 (45.5)	1.538	.464	–	–	–	–	–	–	–	–	–	–	–	–

BDI-II, Beck Depression Inventory–II; CHR, clinical high risk; CPZE, chlorpromazine equivalents; EHI, Edinburgh Handedness Inventory; GAF, Global Assessment of Functioning; HC, healthy control; PANSS, Positive and Negative Syndrome Scale; ROD, recent-onset depression; ROP, recent-onset psychosis.

[a]χ^2 value.

gender distributions of the participants, with the ROP group comprising fewer male participants than the ROD group ($p_{ROP\text{-}ROD}$ = .005), the HC group containing a lower proportion of male participants than both the CHR and ROP groups ($p_{HC\text{-}CHR}$ = .044, $p_{HC\text{-}ROP} < .001$), and the mean age of participants in the CHR group lower than in all other groups ($p_{HC\text{-}CHR}$ = .010, $p_{CHR\text{-}ROP}$ = .013, $p_{CHR\text{-}ROD}$ = .011). Significant differences between the groups were also present in the clinical scores and medication dose, although the CHR and ROD groups did not differ significantly in any feature except the positive symptom domain of the PANSS. Participants were recruited from 7 research centers. The highest number of patients were tested at the Munich (n = 179) and Cologne (n = 123) centers, with additional participants included from the Basel (n = 92), Udine (n = 88), Birmingham (n = 69), Turku (n = 78), and Milan (n = 41) centers. The distribution of participants by group differed significantly between several of the sites (Table S1).

Identification of FC Brain States

We tested the robustness of the clustering procedure by applying it separately to the first and second halves of the scans of HC participants and by varying the number of clusters obtained by the algorithm. In the analysis of the split-half fMRI time series (Figure S1A), multiple states correlated very highly between halves, regardless of the number of states k considered. For k < 4, all correlations of matching states identified in separate halves were higher than the maximum correlation between separate states identified in the same half of the data. For partition models with more clusters, the correlations between some of the matching states remained robust, while other states were less similar to their closest equivalent in the other halves of the scans. For k = 5, all but one of the states were highly consistent, and the state with the lowest consistency still correlated more strongly between halves than in most of the other partition models. While the Caliński-Harabasz score did not suggest a particular number of states to be ideal, the solutions with 5, 7, and 10 states exhibited particularly low Davies-Bouldin scores (Figure S1B, C). Since the model yielding 5 clusters performed well with respect to both the split-half consistency and the clustering score, we selected it for further analysis.

The 5 distinct FC patterns of the brain states we obtained for each diagnostic group are shown in Figure 2A. States identified in the patient groups were matched to their closest HC state, with the correlations of the states between groups presented in Figure 2B. The means of states 2, 4, and 5 were highly consistent between groups, indicating that these states could be identified robustly in all patients and HC participants. State 1 exhibited slightly lower correlations in its mean between the HC, CHR, and ROD groups, with the ROP group mean diverging from all 3 groups. The mean of state 3 exhibited a high correlation between the HC and CHR groups but low correlations in the other group comparisons.

For each HC state, we computed average connectivities in and between functional networks identified by Dosenbach *et al.* (48) (Figure 2C, D). State 1 was characterized by disconnectivity between the sensorimotor and cingulo-opercular networks as well as DMNs and connectivity within the areas belonging to the DMN and cingulo-opercular network. Within-network and between-network connectivities in almost all regions were high in state 2. The cerebellum network and the DMN were strongly connected in state 3, with disconnectivity between the cerebellar network and the sensorimotor network as well as the DMN. States 4 and 5 displayed particularly low connectivities both within and between networks, with cingulo-opercular and sensorimotor connectivity, as well as sensorimotor-cerebellar disconnectivity, higher in state 4.

Group-Level Differences in Dynamic Parameters of FC States

Lifetimes and frequencies of each state in each group after transformation to a Gaussian distribution and confound regression are displayed in Figure 3A and B. States 4 and 5, which showed the highest correspondence across groups, also occurred with the highest frequency: State 5 was active for approximately 50% of the time, and state 4 was active between 18% and 30% of the time. The other states each accounted for less than 20% of the total time. Similarly, state 5 exhibited the longest average lifetime, and state 4 exhibited the second longest average lifetime (Table S3). Significant differences between groups emerged in all states. Participants in the ROD group spent less total time in state 2 than participants in the HC and ROP groups. They also exhibited higher frequencies than participants in the other groups and longer lifetimes than participants in the HC and ROP groups in state 5. In the ROP group, state 1 was active for longer in total than in the CHR and ROD groups and for longer lifetimes than in the 3 other groups. All patient groups experienced state 4 for longer lifetimes than the HC group. The ROP group showed higher frequencies in this state than HC and ROD groups. For state 3, all group differences except those between the HC and CHR groups in both parameters were significant, although the extent of the differences was relatively small. In addition, wide distributions could be observed for multiple groups and states across both parameters, suggesting a high level of between-participant variability.

The analysis of state transitions (Figure 4) showed that across the diagnostic groups, the majority of states transitioned most often into state 5, the most common and longest-lasting state in each group. From state 5, the transition into state 4 was most frequent in each group, although the frequency was increased in the ROP and ROD groups. Transitions from state 5 to states 2 and 3 were also common in the HC and CHR groups. The other groups transitioned into state 2 roughly a quarter of the time, with the other transitions much less common. In the HC and CHR groups, transitions from state 4 into state 3 were also particularly common, whereas they were less frequent in the ROD group and rare in the ROP group. The in-degree of patients in the ROD group was significantly lower than that of patients in the ROP group for state 1 and significantly higher for state 2. The transition behavior of state 3 was fairly inconsistent, with significant differences in the in-degree between most groups.

Association Between dFC and Clinical Characteristics

CCA identified 2 sets of linear combinations of dFC features that correlated significantly with linear combinations of clinical

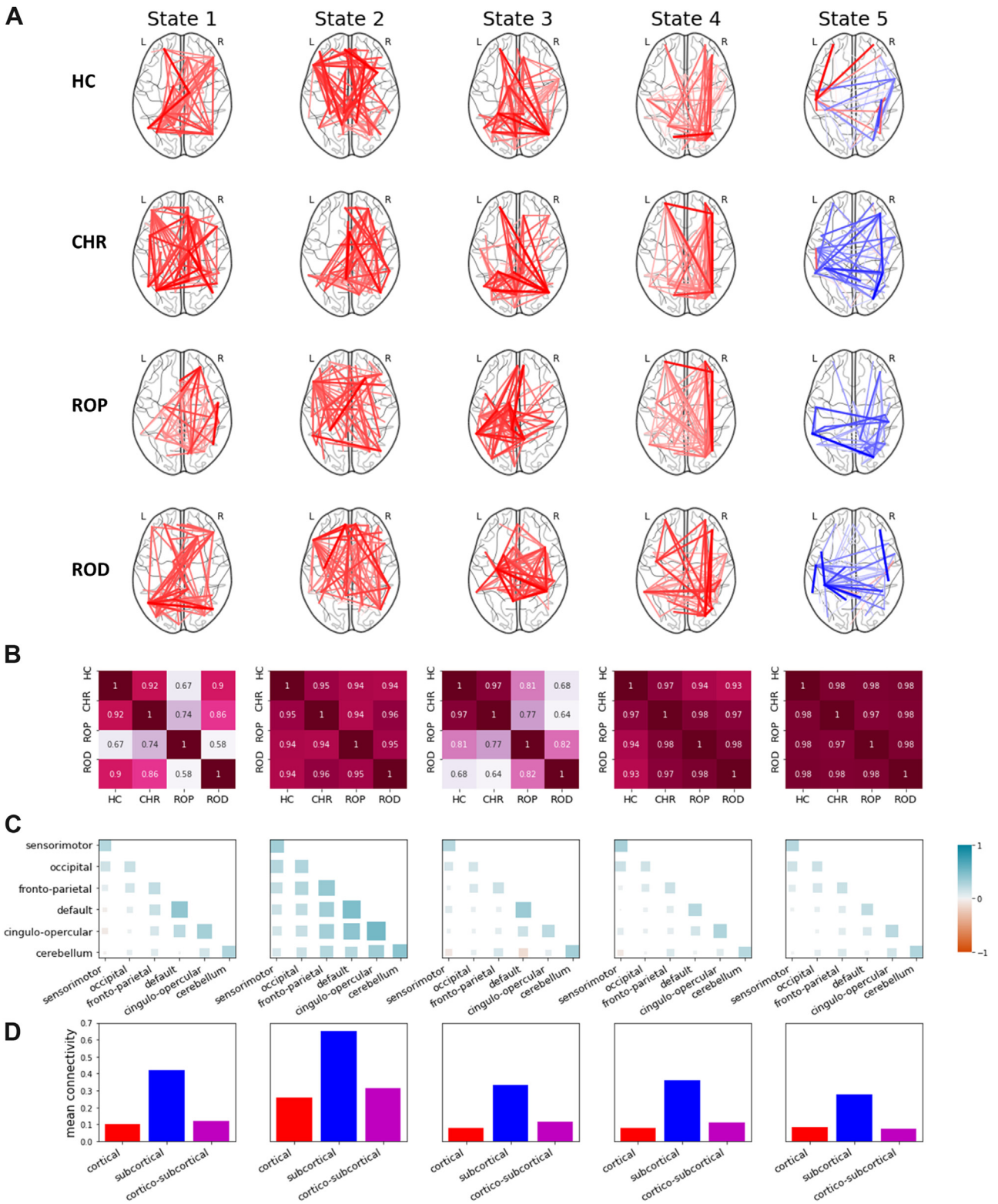

Figure 2. Unique functional connectivity patterns identified by k-means clustering (k = 5). **(A)** Network representation of functional connectivity states across diagnostic groups. For each group, the difference in distributions of connectivity values between matrices assigned to a given state and the remaining data points were evaluated using a Mann-Whitney test. Nonsignificant effects ($p < .05/[12{,}720 \times k]$) were disregarded, and the top 5% of connections with the largest effect sizes are displayed. Red lines indicate positive connectivity values, and blue lines indicate negative connectivity values. **(B)** Correlation matrix of

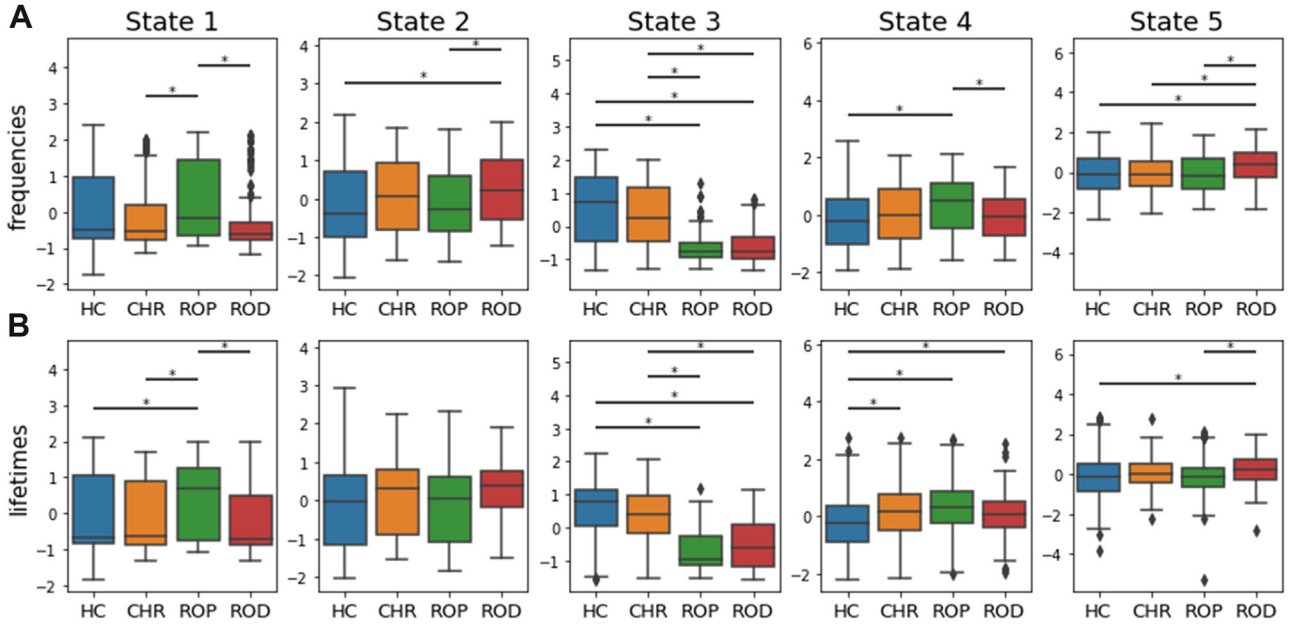

Figure 3. Groupwise comparison of dynamic functional connectivity parameters. **(A)** Frequencies and **(B)** lifetimes of each state for each group after normalization and confound regression. *Significant differences after Bonferroni correction ($p < .0016$). Effect sizes and p values are listed in Tables S2 and S3. CHR, clinical high risk; HC, healthy control; ROD, recent-onset depression; ROP, recent-onset psychosis.

variables. The loadings, the correlation of each feature with the respective component, and the relationship between dFC and clinical component values are shown in Figure 5. The first clinical component was highly associated with positive symptom severity as well as medication dose. The corresponding dFC component exhibited a strong positive correlation with the frequency of states 1, 4, and 5, in addition to the lifetime of state 5 and the transition from state 5 to state 3. This mode achieved a degree of separation of diagnostic groups, with the ROP group scoring higher in both dimensions than the CHR and ROD groups and the CHR group scoring slightly higher in the clinical component than the ROD group. Two other modes, one of which was associated in particular with the PANSS general score, also appeared to be significant, but did not survive Bonferroni correction for multiple comparisons (Figure S2).

DISCUSSION

In this study, we aimed to characterize common and unique alterations of dFC in psychosis and depression. We computed dynamic parameters of FC states in CHR, ROP, and ROD groups as well as an HC group; compared those features between the groups; and associated them with clinical, demographic, and cognitive variables.

Across the diagnostic groups, the states identified overlapped substantially. The means of the more prevalent states 2, 4, and 5 correlated strongly between all groups and displayed similar state-specific connectivity patterns, indicating that brain dynamics in all 4 groups are characterized by alternations between the same set of brain states. States 1 and 3, which occurred least frequently, differed in their means between groups. In addition, the split-half analysis was able to identify a majority of states that were consistent between the datasets regardless of the number of states considered, and the 7-state clustering solution yielded several states that matched those identified with k = 5, confirming the robustness of the 5 states we used for further analysis.

The group-level comparisons of dFC parameters revealed several significant differences between the diagnostic groups. All patient groups exhibited increased lifetimes in state 4, which encompassed low connectivities both within and between networks, with higher values in the sensorimotor and cingulo-opercular networks. The ROP group also showed a higher frequency of this state than the HC and ROD groups. This increase in the total time spent in state 4 is likely related to the abnormally high transition frequency from state 5, the most common state, into state 4, which was specific to patients with ROP. Since increased synchronization in both the sensorimotor and the cingulo-opercular networks has been linked to excess dopamine (58), this finding highlights a potential role of dopamine signaling disturbances, which have long been considered a key mechanism in psychosis (59–61), in dFC alterations in patients with ROP. Research has not identified the same abnormalities in the dopamine signaling pathway in patients with depression (62), suggesting that the common

state means between groups. **(C)** Mean connectivities within and between resting-state networks. Square sizes represent absolute values. **(D)** Mean connectivities within and between cortical and subcortical areas. CHR, clinical high risk; HC, healthy control; L, left; R, right, ROD, recent-onset depression; ROP, recent-onset psychosis.

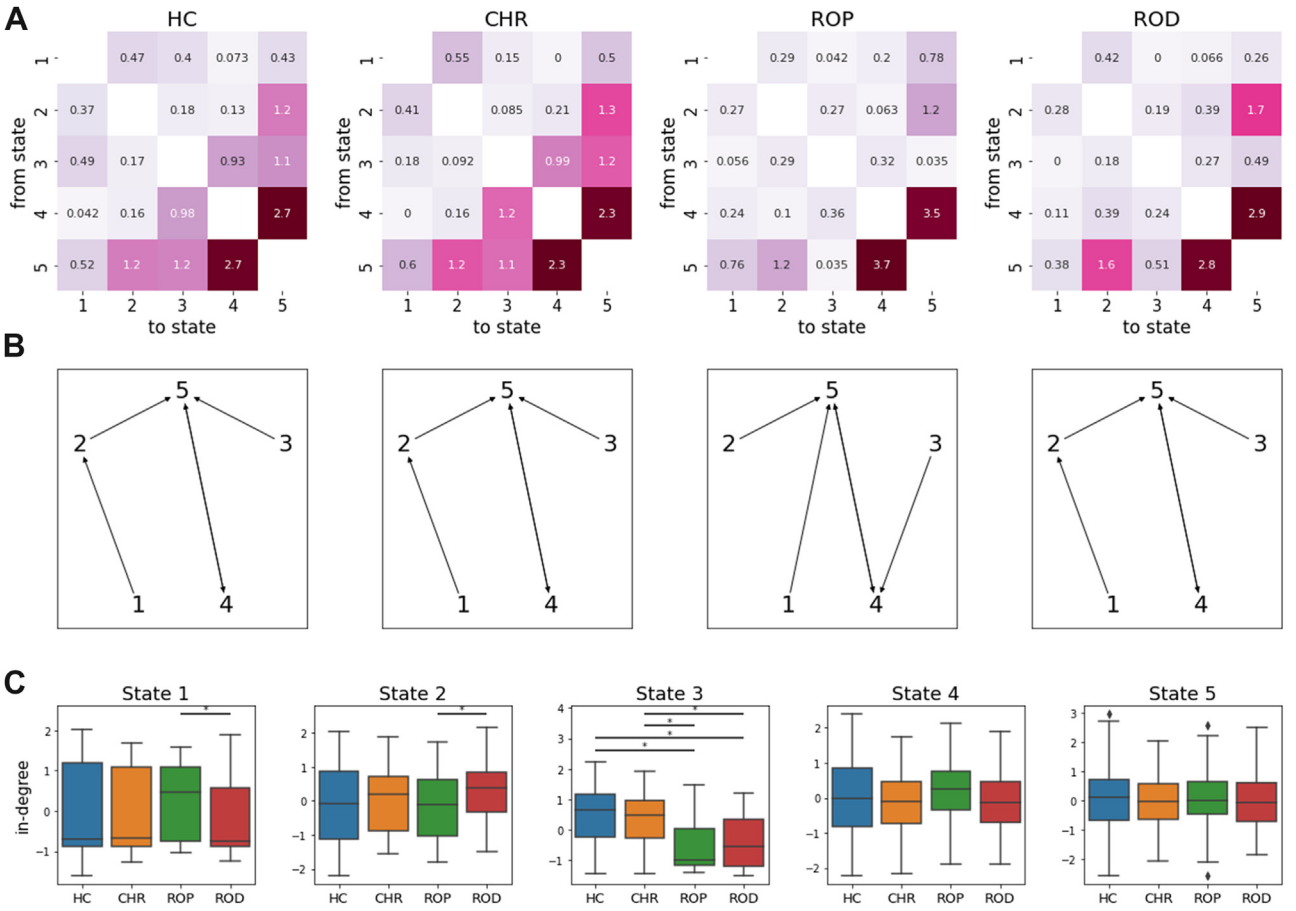

Figure 4. State transitions. **(A)** Transition matrix showing the average number of switches between each pair of states. **(B)** Graph representation considering only the most common transition out of each state. **(C)** In-degree of each state. *Significant differences after Bonferroni correction ($p < .0016$). Effect sizes and p values are listed in Table S4. CHR, clinical high risk; HC, healthy control; ROD, recent-onset depression; ROP, recent-onset psychosis.

increase in lifetime in this state is not linked to this system. Further research is necessary to determine whether there is a common mechanism contributing to the increase in lifetime across all groups or whether this is a common effect caused by distinct processes.

In the ROD group, state 5, the most common state featuring low connectivities within and between most networks, was active for significantly longer durations than in the other groups. These findings match those of previous analyses of dFC in patients with depression, which have shown an

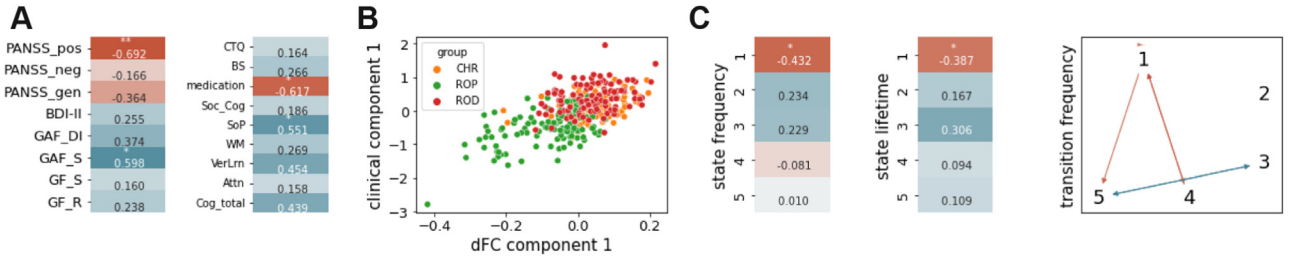

Figure 5. Significantly correlated mode identified by canonical correlation analysis. **(A)** Clinical variable loadings. **(B)** Scatter plot of clinical component values in relation to dynamic functional connectivity (dFC) component values. **(C)** Dynamic functional connectivity feature loadings. In the heatmaps, stars indicate significance before and after Bonferroni correction. *$p < .05$; **$p < .0029$. Only transition frequencies with significant loadings ($p < .05$) are displayed. Attn, attention; BDI-II, Beck Depression Inventory–II; BS, Bullying Scale; Cog_total, total cognition score; CTQ, Childhood Trauma Questionnaire; GAF_DI, Global Assessment of Functioning Disability/Impairment; GAF_S, GAF Symptoms; GF_R, Global Functioning: Role Scale; GF_S, GF: Social Scale; PANSS_gen, Positive and Negative Syndrome Scale General Scale; PANSS_neg, PANSS Negative Scale; PANSS_pos, PANSS Positive Scale; Soc_Cog, social cognition; SoP, speed of processing; VerLrn, verbal learning; WM, working memory.

increased lifetime of a weakly connected state (4) and increased temporal stability in FC (33,63), which might result from longer lifetimes of the most common state. The ROD group also showed increased frequencies in the highly connected state 2 compared with the HC and ROP groups. While evidence from dFC studies related to this state is lacking, Schaefer *et al.* (64) found that administration of a selective serotonin reuptake inhibitor leads to a widespread decrease of FC in healthy individuals, suggesting the possibility that the increased lifetime of the highly connected state might be linked to abnormal serotonin signaling reported in patients with depression (65).

The investigation of the links between these dynamic FC measures and clinical variables via CCA in the CHR, ROP, and ROD groups revealed several significantly correlated canonical variates. The strongest association was discovered between positive psychosis symptom severity and antipsychotic medication dose and dFC parameters of several states. The ROP group could be separated along these 2 dimensions from the CHR and ROD groups, which overlapped. Since the severity of positive psychosis symptoms is one of the main clinical factors distinguishing between the groups, it is not surprising that a component dominated by this feature would yield the clearest separation between any of the groups. Past research has found evidence of an association between the PANSS positive scale and static FC measures (66,67). The fact that medication dose was significantly correlated with the first canonical variate complicates the interpretation of this association, as research shows that antipsychotic medication can affect brain connectivity (68–70). However, the correlation of the clinical and dFC components of the first mode and the loadings of the PANSS positive scale on the clinical component remained significant even after removing medication effects via confound regression (Figure S5), suggesting that medication dose does not drive positive symptom severity and the shift in dFC parameters independently.

Some limitations of the study methodology should be considered. We analyzed a large sample and were able to produce robust findings with regard to confounds such as age, gender, site, and motion effects (Figures S3, S4), but included only data from a single study in our investigation. Thus, testing the methodology on additional, unseen data to validate these results is advisable. One of the factors particularly susceptible to variations in the dataset or analysis methodology appears to be the number of states k, with the chosen value varying across studies (4,53,71). When we repeated the analysis with a different number of states, many, but not all, of our results remained consistent (Figure S6), suggesting that a further validation of these findings is advisable.

As the scope of the present study is limited to the clinical factors we incorporated in the analysis, future studies could expand on these findings by supplementing them with additional variables. By including follow-up data, clinical value would be added to such an analysis. To further elucidate mechanisms of the CHR stage and the progression to psychosis, a stratification of patients at CHR for psychosis based on long-term outcomes is necessary. For patients with ROD and patients with ROP, consideration of outcomes would allow for an analysis of potential risk and resilience factors. The association of dFC parameters with other biological, behavioral, and clinical information, such as genetics, lifestyle choices, and symptom profiles, would further enrich our understanding of the mechanisms of psychiatric disorders and individual variability. In addition, a more thorough investigation of the less common states 1 and 3 could reveal important information on brain changes in psychotic and depressive disorders. While they are group-specific features of the dFC landscape, their lack of consistency between the groups limits the interpretability of their dFC parameters. The smaller, less consistent clusters might constitute intermediate states, highlight abnormalities within some of the more consistent states, or represent states unique to particular groups altogether. Additional analyses able to better separate clusters of unequal sizes, and achieve higher temporal resolution, are necessary for future investigation of this issue.

In this study, we found abnormalities in dFC in patients with depression and patients with psychosis. The dFC parameters were associated with both psychosis symptoms and transdiagnostic factors. These results indicate specific alterations in brain communication in patients diagnosed with depression and psychosis and show that individual variability across positive psychosis symptom severity is represented in brain connectivity dynamics. Future studies should investigate how changes in dFC parameters relate to the risk of conversion to psychosis in patients with CHR for psychosis.

ACKNOWLEDGMENTS AND DISCLOSURES

This work was supported by the Deutsche Forschungsgemeinschaft (DFG; German Research Foundation) (Grant Nos. Project-ID 431549029, SFB 1451, and 491111487) and Koeln Fortune Program/Faculty of Medicine, University of Cologne (Grant No. 370/2020 [to TL]). The PRONIA study is a Collaboration Project funded by the European Union under the Seventh Framework Programme (Grant Agreement No. 602152).

The PRONIA Consortium: The collaborators listed here performed the screening, recruitment, rating, examination, and follow-up of the study participants. They were involved in implementing the examination protocols of the study, setting up its information technology infrastructure, and organizing the flow and quality control of the data analyzed in this article between the local study sites and the central study database.

Linda Betz, Anne Erkens, Eva Gussmann, Shalaila Haas, Alkomiet Hasan, Claudius Hoff, Ifrah Khanyaree, Aylin Melo, Susanna Muckenhuber-Sternbauer, Janis Köhler, Ömer Öztürk, Nora Penzel, David Popovic, Adrian Rangnick, Sebastian von Saldern, Rachele Sanfelici, Moritz Spangemacher, Ana Tupac, Maria Fernanda Urquijo, Johanna Weiske, and Antonia Wosgien (Department of Psychiatry and Psychotherapy, Ludwig-Maximilian-University, Munich, Germany).

Karsten Blume, Dominika Gebhardt, Nathalie Kaiser, Ruth Milz, Alexandra Nikolaides, Mauro Seves, Silke Vent, and Martina Wassen (Department of Psychiatry and Psychotherapy, University of Cologne, Cologne, Germany).

Christina Andreou, Laura Egloff, Fabienne Harrisberger, Claudia Lenz, Letizia Leanza, Amatya Mackintosh, Renata Smieskova, Erich Studerus, Anna Walter, and Sonja Widmayer (Department of Psychiatry, Psychiatric University Hospital, University of Basel, Basel, Switzerland).

Chris Day, Mariam Iqbal, Mirabel Pelton, Pavan Mallikarjun, Alexandra Stainton, and Ashleigh Lin (Institute for Mental Health and School of Psychology, University of Birmingham, United Kingdom).

Alexander Denissoff, Anu Ellilä, Tiina From, Markus Heinimaa, Tuula Ilonen, Päivi Jalo, Heikki Laurikainen, Antti Luutonen, Akseli Mäkela, Janina Paju, Henri Pesonen, Reetta-Liina Säilä, Anna Toivonen, and Otto Turtonen (Department of Psychiatry, University of Turku, Finland).

Ana Beatriz Solana, Manuela Abraham, Nicolas Hehn, and Timo Schirmer (GE Global Research, Niskayuna, New York).

Carlo Altamura, Marika Belleri, Francesca Bottinelli, Adele Ferro, and Marta Re (Workgroup of Paolo Brambilla, Department of Neuroscience and

Mental Health, Fondazione IRCCS Ca'Granda Ospedale Maggiore Policlinico, University of Milan, Milan, Italy).

Emiliano Monzani and Maurizio Sberna (Programma2000, Niguarda Hospital, Milan, Italy).

Armando D'Agostino and Lorenzo Del Fabro (Workgroup of Paolo Brambilla, San Paolo Hospital, Milan, Italy).

Giampaolo Perna, Maria Nobile, and Alessandra Alciati (Workgroup of Paolo Brambilla, Villa San Benedetto Menni, Albese con Cassano, Italy).

Matteo Balestrieri, Carolina Bonivento, Giuseppe Cabras, and Franco Fabbro (Workgroup of Paolo Brambilla, Department of Medical Area, University of Udine, Udine, Italy).

Marco Garzitto and Sara Piccin (Workgroup of Paolo Brambilla, IRCCS Scientific Institute "E. Medea," Polo del Friuli Venezia Giulia, Udine, Italy).

NK received honoraria for talks presented at education meetings organized by Otsuka/Lundbeck. RU reports grants from the Medical Research Council, grants from the National Institute for Health Research: Health Technology Assessment, grants from the European Commission–Research: The Seventh Framework Programme, and personal speaker fees from Sunovion, outside the submitted work. RL participated in advisory boards and received honoraria for talks presented at educational meetings organized by Janssen-Cilag, Otsuka/Lundbeck, and ROVI outside the submitted work. JK received honoraria for talks presented at education meetings organized by Janssen and Otsuka/Lundbeck. All other authors report no biomedical financial interests or potential conflicts of interest.

ARTICLE INFORMATION

From Cognitive Neuroscience (INM-3), Institute of Neurosciences and Medicine, Forschungszentrum Jülich, Jülich, Germany (LH, GRF, SD, JK); Department of Psychiatry and Psychotherapy, Faculty of Medicine and University Hospital, University of Cologne, Cologne, Germany (LH, LK-I, JW, TL, MR, SR, JK); Department of Psychiatry and Psychotherapy, Ludwig Maximilians University, Munich, Germany (LK-I, AR, NK); Department of Psychiatry, Icahn School of Medicine at Mount Sinai, New York, New York (SSH); Department of Translational Biomedicine and Neuroscience, University of Bari Aldo Moro, Bari, Italy (LAA); Department of Psychiatry, Massachusetts General Hospital, Harvard Medical School, Boston, Massachusetts (NP); Department of Psychiatry and Psychotherapy, University of Düsseldorf, Düsseldorf, Germany (FS-L, EM); University Hospital of Child and Adolescent Psychiatry and Psychotherapy, University of Bern, Bern, Switzerland (FS-L); Department of Psychology and Mental Health, Faculty of Psychology, Airlangga University, Surabaya, Indonesia (FS-L); Centre for Youth Mental Health, University of Melbourne, Parkville, Victoria, Australia (DBD, SJW); Orygen, Parkville, Victoria, Australia (DBD, SJW); Department of Psychiatry, University of Turku, Turku, Finland (RKRS); Institute for Translational Psychiatry, University of Münster, Münster, Germany (RL); Department of Psychiatry and Psychotherapy, Lübeck University, Lübeck, Germany (RL, SB); Department of Pathophysiology and Transplantation, University of Milan, Milan, Italy (PB); Department of Neurosciences and Mental Health, IRCCS Ca' Granda Ospedale Maggiore Policlinico, Milan, Italy (PB); Institute for Mental Health, University of Birmingham, Birmingham, United Kingdom (SJW, RU); Centre for Human Brain Health, University of Birmingham, Birmingham, United Kingdom (RU); Birmingham Early Interventions Service, Birmingham Women's and Children's NHS Foundation Trust, Birmingham, United Kingdom (RU); Department of Basic Medical Science, Neuroscience, and Sense Organs, University of Bari Aldo Moro, Bari, Italy (AB); Department of Neurology, Faculty of Medicine and University Hospital, University of Cologne, Cologne, Germany (GRF); Institute of Zoology, University of Cologne, Cologne, Germany (SD).

Address correspondence to Joseph Kambeitz, M.D., at Joseph.Kambeitz@uk-koeln.de.

Received Nov 30, 2023; revised Jan 23, 2024; accepted Feb 15, 2024.

Supplementary material cited in this article is available online at https://doi.org/10.1016/j.bpsc.2024.02.013.

REFERENCES

1. Vos T, Lim SS, Abbafati C, Abbas KM, Abbasi M, Abbasifard M, *et al.* (2020): Global burden of 369 diseases and injuries in 204 countries and territories, 1990–2019: A systematic analysis for the Global Burden of Disease Study 2019. Lancet 396:1204–1222.
2. Fusar-Poli P, Correll CU, Arango C, Berk M, Patel V, Ioannidis JPA (2021): Preventive psychiatry: A blueprint for improving the mental health of young people. World Psychiatry 20:200–221.
3. Wise T, Cleare AJ, Herane A, Young AH, Arnone D (2014): Diagnostic and therapeutic utility of neuroimaging in depression: An overview. Neuropsychiatr Dis Treat 10:1509–1522.
4. Yao Z, Shi J, Zhang Z, Zheng W, Hu T, Li Y, *et al.* (2019): Altered dynamic functional connectivity in weakly-connected state in major depressive disorder. Clin Neurophysiol 130:2096–2104.
5. Damaraju E, Allen EA, Belger A, Ford JM, McEwen S, Mathalon DH, *et al.* (2014): Dynamic functional connectivity analysis reveals transient states of dysconnectivity in schizophrenia. Neuroimage Clin 5:298–308.
6. Thomas Yeo BT, Krienen FM, Sepulcre J, Sabuncu MR, Lashkari D, Hollinshead M, *et al.* (2011): The organization of the human cerebral cortex estimated by intrinsic functional connectivity. J Neurophysiol 106:1125–1165.
7. Raichle ME (2011): The restless brain. Brain Connect 1:3.
8. Zhang J, Kucyi A, Raya J, Nielsen AN, Nomi JS, Damoiseaux JS, *et al.* (2021): What have we really learned from functional connectivity in clinical populations? Neuroimage 242:118466.
9. Fox M, Greicius M (2010): Clinical applications of resting state functional connectivity. Front Syst Neurosci 4:19.
10. Del Fabro L, Schmidt A, Fortea L, Delvecchio G, D'Agostino A, Radua J, *et al.* (2021): Functional brain network dysfunctions in subjects at high-risk for psychosis: A meta-analysis of resting-state functional connectivity. Neurosci Biobehav Rev 128:90–101.
11. Hubl D, Schultze-Lutter F, Hauf M, Dierks T, Federspiel A, Kaess M, *et al.* (2018): Striatal cerebral blood flow, executive functioning, and fronto-striatal functional connectivity in clinical high risk for psychosis. SchizophrRes 201:231–236.
12. Langhein M, Lyall AE, Steinmann S, Seitz-Holland J, Nägele FL, Cetin-Karayumak S, *et al.* (2022): The decoupling of structural and functional connectivity of auditory networks in individuals at clinical high-risk for psychosis. World J Biol Psychiatry 24:387–399.
13. Fusar-Poli P, Salazar de Pablo G, Correll CU, Meyer-Lindenberg A, Millan MJ, Borgwardt S, *et al.* (2020): Prevention of psychosis: advances in detection, prognosis, and intervention. JAMA Psychiatry 77:755–765.
14. Wood SJ, Yung AR, McGorry PD, Pantelis C (2011): Neuroimaging and treatment evidence for clinical staging in psychotic disorders: From the at-risk mental state to chronic schizophrenia. Biol Psychiatry 70:619–625.
15. Kaiser RH, Andrews-Hanna JR, Wager TD, Pizzagalli DA (2015): Large-scale network dysfunction in major depressive disorder: Meta-analysis of resting-state functional connectivity. JAMA Psychiatry 72:603–611.
16. Mulders PC, van Eijndhoven PF, Schene AH, Beckmann CF, Tendolkar I (2015): Resting-state functional connectivity in major depressive disorder: A review. Neurosci Biobehav Rev 56:330–344.
17. Kambeitz J, Kambeitz-Ilankovic L, Cabral C, Dwyer DB, Calhoun VD, van den Heuvel MP, *et al.* (2016): Aberrant functional whole-brain network architecture in patients with schizophrenia: A meta-analysis. Schizophr Bull 42(Suppl 1):S13–S21.
18. Lynall M-E, Bassett DS, Kerwin R, McKenna PJ, Kitzbichler M, Muller U, *et al.* (2010): Functional connectivity and brain networks in schizophrenia. J Neurosci 30:9477–9487.
19. Shao J, Meng C, Tahmasian M, Brandl F, Yang Q, Luo G, *et al.* (2018): Common and distinct changes of default mode and salience network in schizophrenia and major depression. Brain Imaging Behav 12:1708–1719.
20. Yang Y, Liu S, Jiang X, Yu H, Ding S, Lu Y, *et al.* (2019): Common and specific functional activity features in schizophrenia, major depressive disorder, and bipolar disorder. Front Psychiatry 10:52.
21. Dong D, Wang Y, Chang X, Luo C, Yao D (2018): Dysfunction of large-scale brain networks in schizophrenia: A meta-analysis of resting-state functional connectivity. Schizophr Bull 44:168–181.
22. Furman DJ, Hamilton JP, Gotlib IH (2011): Frontostriatal functional connectivity in major depressive disorder. Biol Mood Anxiety Disord 1:11.
23. Karcher NR, Rogers BP, Woodward ND (2019): Functional connectivity of the striatum in schizophrenia and psychotic bipolar disorder. Biol Psychiatry Cogn Neurosci Neuroimaging 4:956–965.

24. Hua JPY, Karcher NR, Merrill AM, O'Brien KJ, Straub KT, Trull TJ, *et al.* (2019): Psychosis risk is associated with decreased resting-state functional connectivity between the striatum and the default mode network. Cogn Affect Behav Neurosci 19:998–1011.
25. Weber S, Johnsen E, Kroken RA, Løberg E-M, Kandilarova S, Stoyanov D, *et al.* (2020): Dynamic functional connectivity patterns in schizophrenia and the relationship with hallucinations. Front Psychiatry 11:227.
26. Barber AD, Lindquist MA, DeRosse P, Karlsgodt KH (2018): Dynamic functional connectivity states reflecting psychotic-like experiences. Biol Psychiatry Cogn Neurosci Neuroimaging 3:443–353.
27. Du Y, Fryer SL, Fu Z, Lin D, Sui J, Chen J, *et al.* (2018): Dynamic functional connectivity impairments in early schizophrenia and clinical high-risk for psychosis. Neuroimage 180:632–645.
28. Preti MG, Bolton TA, Van De Ville D (2017): The dynamic functional connectome: State-of-the-art and perspectives. Neuroimage 160:41–54.
29. Hutchison RM, Womelsdorf T, Allen EA, Bandettini PA, Calhoun VD, Corbetta M, *et al.* (2013): Dynamic functional connectivity: Promise, issues, and interpretations. Neuroimage 80:360–378.
30. Fu Z, Iraji A, Sui J, Calhoun VD (2021): Whole-brain functional network connectivity abnormalities in affective and non-affective early phase psychosis. Front Neurosci 15:682110.
31. Zhang Z, Zhuo K, Xiang Q, Sun Y, Suckling J, Wang J, *et al.* (2021): Dynamic functional connectivity and its anatomical substrate reveal treatment outcome in first-episode drug-naïve schizophrenia. Transl Psychiatry 11:1–12.
32. Wang J, Wang Y, Huang H, Jia Y, Zheng S, Zhong S, *et al.* (2020): Abnormal dynamic functional network connectivity in unmedicated bipolar and major depressive disorders based on the triple-network model. Psychol Med 50:465–474.
33. Demirtaş M, Tornador C, Falcón C, López-Solà M, Hernández-Ribas R, Pujol J, *et al.* (2016): Dynamic functional connectivity reveals altered variability in functional connectivity among patients with major depressive disorder. Hum Brain Mapp 37:2918–2930.
34. Sun Y, Collinson SL, Suckling J, Sim K (2019): Dynamic reorganization of functional connectivity reveals abnormal temporal efficiency in schizophrenia. Schizophr Bull 45:659–669.
35. Koutsouleris N, Dwyer DB, Degenhardt F, Maj C, Urquijo-Castro MF, Sanfelici R, *et al.* (2021): Multimodal machine learning workflows for prediction of psychosis in patients with clinical high-risk syndromes and recent-onset depression. JAMA Psychiatry 78:195–209.
36. Koutsouleris N, Kambeitz-Ilankovic L, Ruhrmann S, Rosen M, Ruef A, Dwyer DB, *et al.* (2018): Prediction models of functional outcomes for individuals in the clinical high-risk state for psychosis or with recent-onset depression: A multimodal, multisite machine learning analysis. JAMA Psychiatry 75:1156–1172.
37. First MB, Spitzer RL, Gibbon M, Williams JBW (2002): Structured Clinical Interview DSM-IV-TR Axis I Disorders, Research Version, Patient Edition (SCID-I/P). New York: Biometrics Research, New York State Psychiatric Institute.
38. Schultze-Lutter F, Addington J, Ruhrmann S, Klosterkötter J (2007): Schizophrenia Proneness Instrument, Adult Version (SPI-A). Rome: Giovanni Fioriti Editore.
39. McGlashan T, Walsh B, Woods S (2010): The Psychosis Risk Syndrome: Handbook for Diagnosis and Follow-Up. Oxford: Oxford University Press.
40. Beck AT, Steer RA, Ball R, Ranieri W (1996): Comparison of Beck Depression Inventories -IA and -II in psychiatric outpatients. J Pers Assess 67:588–597.
41. Kay SR, Fiszbein A, Opler LA (1987): The Positive and Negative Syndrome Scale (PANSS) for schizophrenia. Schizophr Bull 13:261–276.
42. Niendam TA, Bearden CE, Johnson JK, Cannon TD (2006): Global Functioning: Role Scale (GF: Role). Los Angeles: University of California, Los Angeles.
43. Auther AM, Smith CW, Cornblatt BA (2006): Global Functioning: Social Scale (GF: Social). Glen Oaks, NY: Zucker Hillside Hospital.
44. Pedersen G, Hagtvet KA, Karterud S (2007): Generalizability studies of the Global Assessment of Functioning-Split version. Compr Psychiatry 48:88–94.
45. Haas SS, Antonucci LA, Wenzel J, Ruef A, Biagianti B, Paolini M, *et al.* (2021): A multivariate neuromonitoring approach to neuroplasticity-based computerized cognitive training in recent onset psychosis. Neuropsychopharmacology 46:828–835.
46. Patel AX, Kundu P, Rubinov M, Jones PS, Vértes PE, Ersche KD, *et al.* (2014): A wavelet method for modeling and despiking motion artifacts from resting-state fMRI time series. Neuroimage 95:287–304.
47. Power JD, Mitra A, Laumann TO, Snyder AZ, Schlaggar BL, Petersen SE (2014): Methods to detect, characterize, and remove motion artifact in resting state fMRI. Neuroimage 84:320–341.
48. Dosenbach NUF, Nardos B, Cohen AL, Fair DA, Power JD, Church JA, *et al.* (2010): Prediction of individual brain maturity using fMRI. Science 329:1358–1361.
49. Hutchison RM, Womelsdorf T, Gati JS, Everling S, Menon RS (2012): Resting-state networks show dynamic functional connectivity in awake humans and anesthetized macaques. Hum Brain Mapp 34:2154–2177.
50. Leonardi N, Van De Ville D (2015): On spurious and real fluctuations of dynamic functional connectivity during rest. Neuroimage 104:430–436.
51. Zalesky A, Breakspear M (2015): Towards a statistical test for functional connectivity dynamics. Neuroimage 114:466–470.
52. Allen EA, Damaraju E, Plis SM, Erhardt EB, Eichele T, Calhoun VD (2014): Tracking whole-brain connectivity dynamics in the resting state. Cereb Cortex 24:663–676.
53. Snyder W, Uddin LQ, Nomi JS (2021): Dynamic functional connectivity profile of the salience network across the life span. Hum Brain Mapp 42:4740–4749.
54. Davies DL, Bouldin DW (1979): A cluster separation measure. IEEE Transactions on Pattern Analysis and Machine Intelligence 1:224–227.
55. Caliński T, Harabasz J (1974): A dendrite method for cluster analysis. Communications in Statistics 3:1–27.
56. Hotelling H (1936): Relations between two sets of variates. Biometrika 28:321–377.
57. Wang H-T, Smallwood J, Mourao-Miranda J, Xia CH, Satterthwaite TD, Bassett DS, *et al.* (2020): Finding the needle in a high-dimensional haystack: Canonical correlation analysis for neuroscientists. Neuroimage 216:116745.
58. Conio B, Martino M, Magioncalda P, Escelsior A, Inglese M, Amore M, *et al.* (2020): Opposite effects of dopamine and serotonin on resting-state networks: Review and implications for psychiatric disorders. Mol Psychiatry 25:82–93.
59. van Hooijdonk CFM, Drukker M, van de Giessen E, Booij J, Selten J-P, van Amelsvoort TAMJ (2022): Dopaminergic alterations in populations at increased risk for psychosis: A systematic review of imaging findings. Prog Neurobiol 213:102265.
60. Kambeitz J, Abi-Dargham A, Kapur S, Howes OD (2014): Alterations in cortical and extrastriatal subcortical dopamine function in schizophrenia: Systematic review and meta-analysis of imaging studies. Br J Psychiatry 204:420–429.
61. Howes OD, Kambeitz J, Kim E, Stahl D, Slifstein M, Abi-Dargham A, *et al.* (2012): The nature of dopamine dysfunction in schizophrenia and what this means for treatment. Arch Gen Psychiatry 69:776–786.
62. Grace AA (2016): Dysregulation of the dopamine system in the pathophysiology of schizophrenia and depression. Nat Rev Neurosci 17:524–532.
63. Marchitelli R, Paillère-Martinot M-L, Bourvis N, Guerin-Langlois C, Kipman A, Trichard C, *et al.* (2022): Dynamic functional connectivity in adolescence-onset major depression: Relationships with severity and symptom dimensions. Biol Psychiatry Cogn Neurosci Neuroimaging 7:385–396.
64. Schaefer A, Burmann I, Regenthal R, Arélin K, Barth C, Pampel A, *et al.* (2014): Serotonergic modulation of intrinsic functional connectivity. Curr Biol 24:2314–2318.
65. Moncrieff J, Cooper RE, Stockmann T, Amendola S, Hengartner MP, Horowitz MA (2023): The serotonin theory of depression: A systematic umbrella review of the evidence. Mol Psychiatry 28:3243–3256.
66. Tang J, Liao Y, Song M, Gao J-H, Zhou B, Tan C, *et al.* (2013): Aberrant default mode functional connectivity in early onset schizophrenia. PLoS One 8:e71061.

67. Wang D, Li M, Wang M, Schoeppe F, Ren J, Chen H, *et al.* (2020): Individual-specific functional connectivity markers track dimensional and categorical features of psychotic illness. Mol Psychiatry 25:2119–2129.
68. Abbott CC, Jaramillo A, Wilcox CE, Hamilton DA (2013): Antipsychotic drug effects in schizophrenia: A review of longitudinal FMRI investigations and neural interpretations. Curr Med Chem 20:428–437.
69. Sarpal DK, Robinson DG, Lencz T, Argyelan M, Ikuta T, Karlsgodt K, *et al.* (2015): Antipsychotic treatment and functional connectivity of the striatum in first-episode schizophrenia. JAMA Psychiatry 72:5–13.
70. Chopra S, Francey SM, O'Donoghue B, Sabaroedin K, Arnatkeviciute A, Cropley V, *et al.* (2021): Functional connectivity in antipsychotic-treated and antipsychotic-naive patients with first-episode psychosis and low risk of self-harm or aggression: A secondary analysis of a randomized clinical trial. JAMA Psychiatry 78:994–1004.
71. Jiao Z, Gao P, Ji Y, Shi H (2021): Integration and segregation of dynamic functional connectivity states for mild cognitive impairment revealed by graph theory indicators. Contrast Media Mol Imaging: e6890024.